Article:
Alhummiany, BA, Shelley, D, Saysell, M et al. (9 more authors) (2022) Bias and Precision in Magnetic Resonance Imaging-Based Estimates of Renal Blood Flow: Assessment by Triangulation. Journal of Magnetic Resonance Imaging, 55 (4). pp. 1241-1250. ISSN 1053-1807

https://doi.org/10.1002/jmri.27888

Title

Bias and precision in MRI-based estimates of renal blood flow: assessment by triangulation

Authors

Bashair A. Alhummiany, MSc,[1] David Shelley, BSc,[1,2] Margaret Saysell, BSc,[1,2] Maria-Alexandra Olaru, PhD,[3] Bernd Kühn, PhD,[3] David L. Buckley, PhD,[1] Julie Bailey, BSc,[2] Kelly Wroe, BSc,[2] Cherry Coupland, BSc,[2] Michael W. Mansfield, DM,[2] Steven P. Sourbron, PhD,[4] Kanishka Sharma, PhD.[4]

Affiliation

[1] Department of Biomedical Imaging Sciences, University of Leeds, UK.
[2] Leeds Teaching Hospitals NHS Trust, Leeds, UK.
[3] Siemens Healthcare GmbH, Erlangen, Germany.
[4] Department of Imaging, Infection, Immunity and Cardiovascular Disease, The University of Sheffield, UK.

Corresponding author info

Steven P. Sourbron, Email: s.sourbron@sheffield.ac.uk

Grant support

iBEAt study is part of the BEAt-DKD project. The BEAt-DKD project has received funding from the Innovative Medicines Initiative 2 Joint Undertaking under grant agreement No 115974. This Joint Undertaking receives support from the European Union's Horizon 2020 research and innovation programme and EFPIA with JDRF. For a full list of BEAt-DKD partners, see www.beat-dkd.eu

Running title

Triangulation of MRI-based RBF methods

ABSTRACT

Background: Renal blood flow (RBF) can be measured with dynamic contrast enhanced-MRI (DCE-MRI) and arterial spin labelling (ASL). Unfortunately, individual estimates from both methods vary and reference-standard methods are not available. A potential solution is to include a third, arbitrating MRI method in the comparison.

Purpose: To compare RBF estimates between ASL, DCE and phase contrast (PC)-MRI.

Study Type: Prospective.

***Population*:** 25 patients with type-2 diabetes (36% female) and 5 healthy volunteers (HV, 80% female).

***Field Strength/Sequences*:** 3 T; gradient-echo 2D-DCE, pseudo-continuous ASL (pCASL) and cine 2D-PC.

Assessment: ASL, DCE and PC were acquired once in all patients. ASL and PC were acquired four times in each HV. RBF was estimated and split-RBF was derived as (right kidney RBF)/total RBF. Repeatability error (RE) was calculated for each HV, RE=1.96xSD, where SD is standard deviation of repeat scans.

Statistical Tests: Paired t-tests and one-way analysis-of-variance (ANOVA) were used for statistical analysis. The 95% confidence interval (CI) for difference between ASL/PC and DCE/PC was assessed using two-sample *F*-test for variances. Statistical significance level was $p<0.05$. Influential outliers were assessed with Cook's distance ($D_i>1$) and results with outliers removed were presented.

Results: In patients, the mean RBF (mL/min/1.73 m^2) was 618±62 (PC), 526±91 (ASL) and 569±110 (DCE). Differences between measurements were not significant (p=0.28). Intra-subject agreement was poor for RBF with limits-of-agreement

(mL/min/1.73 m^2) [-687, 772] DCE-ASL, [-482, 580] PC-DCE and [-277, 460] PC-ASL. The difference PC-ASL was significantly smaller than PC-DCE, but this was driven by a single-DCE outlier (p=0.31, after removing outlier). The difference in split-RBF was comparatively small. In HVs, mean RE (±95% CI; mL/min/1.73 m^2) was significantly smaller for PC (79±41) than for ASL (241±85).

Conclusions: ASL, DCE and PC RBF show poor agreement in individual subjects but agree well on average. Triangulation with PC suggests that the accuracy of ASL and DCE is comparable.

Key Words: Renal blood flow, arterial spin labelling, dynamic contrast enhanced, phase contrast, kidney

INTRODUCTION

High renal perfusion is essential for sustaining stable glomerular filtration and blood flow autoregulation is vital for protecting the kidney from elevated arterial pressure that causes glomerular capillary injury (1). Impairment in the autoregulatory mechanism of the kidney is known to contribute to diabetic nephropathy (1) and chronic kidney disease (CKD) has been associated with reduced renal perfusion (2). Thus, measurement of renal perfusion can serve as a prognostic biomarker in CKD and aid in the diagnosis of renal dysfunction or in the identification of progressive disease.

MRI enables quantification of renal perfusion (expressed in mL/min/100 mL) either by dynamic contrast enhanced (DCE) (3), or by arterial spin labelling (ASL) (4) based approaches. Both MRI methods have demonstrated promising results for detecting kidney dysfunction and evaluating disease progression (5,6). However, resting perfusion measurements from healthy volunteers reported in the literature vary between the two methods by as much as a factor of two (range between 172 and 427 mL/min/100 mL for cortical perfusion using ASL and between 244 and 443 mL/min/100 mL for the whole parenchyma using DCE, see supplementary file), undermining clinical confidence in MRI perfusion measures. While differences in demographics, subject preparation and physiological variations play a role (7), the effect of measurement error cannot be excluded. Unfortunately, due to the lack of clinical reference standard methods it is not currently possible to distinguish these effects.

In the absence of a reference-standard, comparisons within MRI methods can be performed as an alternative approach. Since DCE and ASL measure renal perfusion based on different mechanisms, it is unlikely that their errors are related. Hence, a strong agreement between the two would offer confidence on the relative accuracy of the techniques. In case of disagreement however, the technical validation will be inconclusive as this could be due to an error in one of the two methods, or in both. Unfortunately, the latter has proven to be the case (8,9); although DCE and ASL have agreed well on average, the limits of agreement are large (10). Other technical validation studies have focused on comparing repeatability and reproducibility of the measurements (7). However, while repeatability is a necessary condition for any assay to be valid, a separate assessment of bias is necessary to avoid promoting methods that are less reliable (11).

A possible approach to assessing bias in the absence of a reference-standard is to involve a third, arbitrating, method. Phase contrast (PC) MRI of the renal arteries is a good candidate as it is built on different physical principles and produces a measurement of renal blood flow (RBF) that can also be derived from ASL and DCE by integrating perfusion values over the parenchyma. Moreover, PC is a well-established method and readily available in clinical practice (12). If PC agrees better with ASL than with DCE for instance, this will offer evidence that ASL is more reliable than DCE (and vice versa). Conversely, if PC agrees equally well with DCE and ASL, this will indicate that DCE and ASL have similar levels of error. Previous work in healthy volunteers has confirmed a significant correlation between ASL and PC (13), but this question has not been addressed in patients and a comparison of all three methods has not yet been performed.

The primary aim of this study was to compare RBF estimates from ASL, DCE and PC in patients with type-2 diabetes. Split RBF (relative to the right kidney, as used in nuclear medicine studies) was also compared between the three methods. In order to support the interpretation of the data, the repeatability of PC and ASL was assessed in healthy volunteers.

METHODS

Subjects

The study was approved by the institutional research ethics committee and written informed consent was obtained from all subjects. The study included 25 consecutive patients with type-2 diabetes (estimated glomerular filtration rate (eGFR) ≥ 30 mL/min/1.73 m^2) from the imaging biomarkers enterprise to attack diabetic kidney disease (iBEAt) study cohort (14). To assess the repeatability of ASL and PC techniques, five healthy volunteers (HVs) underwent four MRI scans. All volunteers were normotensive with no history of diabetes or renal disease.

The same subject preparation and MRI protocol was employed for both patients and HVs, except that DCE was not performed on healthy volunteers. The scans were performed in the morning (between 8-11 am) after an overnight fast (>8 hours). A standard breakfast (containing 2 slices whole bread and butter) and 250 mL of water were provided immediately before the scan. Full details on the iBEAt study including MRI protocol, patient preparation and recruitment criteria have been published previously (14).

Imaging Protocol

MRI data were acquired on a 3 T MRI scanner (MAGNETOM Prisma, Siemens Healthcare GmbH, Erlangen, Germany) using an 18-channel phased array body coil combined with inbuilt spine coil for signal reception. The acquisition involved 2D cine PC-MRI, a prototypical sequence for 3D renal ASL (pseudo-continuous arterial spin labelling (pCASL)) and 2D DCE-MRI sequences acquired in the same order. An overview of the MRI acquisition parameters is listed in Table 1.

PC

The renal arteries were depicted using a combination of a coronal survey scan and an axial half-Fourier acquisition single-shot turbo spin-echo (HASTE) sequence. The imaging plane for PC-MRI was positioned perpendicular to the renal artery close to its origin from the descending aorta.

ASL

Data was recorded using a pseudo-continuous arterial spin labelling (pCASL) sequence with a slice selective labelling pulse. The prototype sequence is implemented by the vendor, and acquires label, control images and a reference proton density weighted (M0) image within the same package (sequence parameters are provided in table 1). The labelling plane was positioned perpendicular to the abdominal aorta 10 cm above the center of the kidneys. Background suppression was employed to reduce signal from static tissue. Perfusion maps were generated on the scanner using inline software, preceded by retrospective 2D motion correction that is applied to the acquired MR datasets using 2D elastic registration. Maps of perfusion rate (in mL/min/100 mL) were derived using the general kinetic model (15).

DCE

Data were acquired continuously using T1-weighted sequence. Gd-DOTA (Dotarem, Guerbet Group, France) was injected intravenously using a quarter dose (0.025 mmol/kg) at a rate of 2 mL/s followed by a 20 mL saline flush. The injection was given using an automatic injector, 20 seconds after the acquisition started.

Post-processing

All post-processing were performed by a radiographer (B.A) with two years of experience in renal MRI analyses.

PC

Analysis was performed on a Syngo.Via workstation (Siemens Healthcare GmbH, Erlangen, Germany). The renal arteries were defined, and threshold adjusted on the anatomical images using an elliptical shape region-of-interest (ROI). The regions were adjusted on each time frame according to renal vessel movement in the cardiac cycle. The ROIs were then propagated automatically into the velocity map images (Figure 1 a and b). Renal blood flow (RBF) was computed by multiplying average blood velocity with average vessel cross-section area reported in units of mL/min.

ASL

Using a prototypical sequence for kidney ASL, perfusion maps were reconstructed on the scanner and exported for analysis. The analysis was performed using PMI 0.4 software (Platform for research in Medical Imaging)(16). The renal parenchyma ROIs were segmented on proton density weighted (M_0) images, using threshold technique based on pixel intensities and transferred to the perfusion map (Figure 1c). Kidney volume (mL) was derived by multiplying the total number of voxels in the ROI by voxel volume and RBF was derived by multiplying the average perfusion of the ROI by its volume.

DCE

Data were also analyzed using PMI 0.4. Breathing motion was corrected using deformable model-driven registration (17). The aorta was defined semi-automatically by setting a user-defined lower threshold on an axial slice of a maximum signal enhancement map. An arterial-input-function (AIF) was derived by averaging the signal values over the ROI. The renal parenchyma was outlined on a map of apparent extracellular volume (mL/100 mL) derived by model-free deconvolution (18). The parenchyma was first coarsely outlined by a manual selection of a lower threshold on this map, followed by manual exclusion of voxels in the renal pelvis,

collecting system or outside the kidney (Figure 1d). A fit was performed to the concentration time curve of the whole parenchyma, which was derived from the signals using a non-linear signal model with a literature-based T1 value of 1200 ms. Tracer-kinetic model fitting was performed with a 2-compartment-filtration model (3).

Reporting

To account for differences in body size between participants, RBF was normalized to body-surface-area (BSA) in units of 1.73 m^2 according to the Du Bois formula (19). RBF reported in this study represents the total RBF of both kidneys obtained as the sum of the right and left RBF. Split RBF was calculated as the ratio of right RBF to total RBF. Measurements are presented as the mean± 95% confidence interval (CI), unless indicated otherwise.

In HVs, the repeatability error (RE) was calculated for each HV as $RE = 1.96 \times SD$ where SD is the standard deviation over the four repeat scans. The *relative* repeatability error (RRE) was calculated as RRE= (RE/mean) x 100% where the mean is the average over repeat scans in the same subject. RE and RRE were subsequently averaged over all 5 volunteers. With these definitions, RE and RRE represent the absolute and relative 95% CI for a measured value in an individual subject, respectively. Population heterogeneity was calculated for the RBF of each method as the standard deviation across the population expressed as a percentage of the population mean.

Statistical Analysis

In patients, repeated measures one-way analysis of variance (ANOVA) and paired t-tests were conducted to determine the significance of the difference in RBF (and split RBF) across the techniques. Influential outliers in the measurements were identified using Cook's distance, with a cut-off value of $D_i > 1$. Where an outlier was deemed influential the results with outliers removed were also provided. The intra-subject agreement in RBF (and split RBF) was assessed using Bland and Altman method (20). A two-sample *F*-test for equal variances was performed to determine the significance of the difference between ASL/PC and DCE/PC. Linear correlations between techniques were assessed using Pearson's correlation coefficient. Statistical significance was defined at $p < 0.05$ for this study.

RESULTS

Participant Demographics

Twenty-five patients (16 males and 9 females, mean age (interquartile range) of 65 (56-72) years) were analyzed and included for comparison. Five healthy volunteers (1 male and 4 females, mean age (interquartile range) of 39 (31-40) years) completed the four visits at an average of 4 months apart (range between 2 to 7 months).

Comparison of ASL, DCE and PC in Diabetic Patients

In patients, whole parenchyma perfusion, averaged over both kidneys, was 146± 22 mL/min/100 mL using ASL and 214± 31 mL/min/100 mL using DCE.

Figure 2 shows the distribution of RBF and split RBF values derived from PC, ASL and DCE in this study. The difference in the means was not significant for RBF (F (1, 32) = 1.26, p = 0.28) or for split RBF (F (2, 36) = 0.14, p=0.87). Using Cook's distance measures, RBF measurement of the subject number 23 was deemed strongly influential (D_i = 4.3). There was no influential outlier for split RBF parameter (D_i < 1 for all data points).

Figure 3 shows Bland Altman analysis for RBF and split RBF pairwise between techniques. For RBF, the plots confirmed a small bias between techniques, but the 95% CI of the differences was large compared to the mean, indicating substantial differences at the subject level. Specifically, the limits-of-agreements for RBF (mL/min/1.73 m^2) were [-687, 772] for DCE-ASL, [-482, 580] for PC-DCE and [-277, 460] for PC-ASL. The 95% CI for the difference was smaller for PC-ASL than PC-DCE, but only marginally significant (p=0.049). Excluding the extreme DCE-RBF outlier (subject 23), the difference was no longer significant (p=0.315), and the limits-

of-agreement were reduced to [-220, 407] for PC-DCE, [-272, 422] for PC-ASL and [-448,411] for DCE-ASL. For split RBF, the plots showed no systematic bias, with the limits-of-agreement of the order [–0.1, 0.1] for each comparison.

Figure 4 show scatterplots for RBF and split RBF pairwise between techniques. Correlations were significant only between PC-ASL for RBF (r =0.57) and between DCE-ASL for split-RBF (r =0.80). Removing the DCE outlier had a small effect on the average RBF measurements, but improved correlations for all techniques ($r \geq 0.41$) as shown in table 2.

Figure 5 shows individual RBF and split RBF values for all patients across the three techniques. An example case is presented in the supplementary Figure S2 shows a typical source of error related to the DCE outlier.

Repeatability of PC and ASL

The average perfusion in the whole parenchyma estimated using ASL in HVs was 155± 50 mL/min/100 mL.

Table 3 summarizes the repeatability results of RBF and split RBF derived from PC and ASL. For RBF, the mean RE of an individual PC measurement was significantly (three times) lower than ASL. The difference in RE between PC and ASL was not significant for split RBF (p=0.35).

When measured with PC, the difference in repeatability between split-RBF and RBF was not significant (RRE 6% vs 11%, p=0.31). Whereas for ASL, split RBF had 5 times better repeatability than RBF (RRE 11% vs 61%).

The difference in the HV population means between PC-RBF and ASL-RBF was relatively large (33%) but not statistically significant (p=0.13). The difference in split-RBF between PC and ASL was much smaller in relative terms (7.8%) and also not

significant (p=0.22). The heterogeneity of the RBF population in ASL (45%) was twice that of PC (21%).

Figure 6 shows the repeat measurements of PC and ASL for each HV. An example case of renal perfusion maps obtained on four repeat scans for the same HV is shown in the supplementary Figure S3.

DISCUSSION

This study compared RBF values between ASL, DCE and PC in diabetic patients. The key finding is that RBF values agree well on average, but intra-subject agreement is poor between all methods. The uncertainty in split RBF is comparatively small, which is consistent with the fact that this metric is a ratio and therefore any scaling errors related to left and right kidney will be eliminated. Therefore, the improved agreement in split RBF suggests that subject-specific scaling errors are responsible for the poorer precision in RBF. The repeatability assessment in healthy volunteers further support the value of PC as a reference method.

With regards to the direct comparison of DCE and ASL, previous studies are not entirely aligned. Cutajar et al. (9) showed that renal perfusion derived from ASL and DCE in healthy humans agreed well on average, but agreement on an individual level was poor with limits-of-agreement of [-150, 200] mL/min/100 g for an individual kidney. Wu et al. (8) on the other hand reported that renal perfusion measurements were correlated but not entirely comparable between ASL and DCE. Our study supports the observation in Cutajar et al. (9) – strengthening the hypothesis that DCE and ASL are unbiased but that one of the two, or both, show poor precision relative to PC.

Comparison with PC in our study indicates that measurement error in both ASL and DCE plays a role, and in an approximately equal measure. In DCE, a possible source of error is inflow effect in the aorta, which varied from case to case. The arterial input function (AIF) of the DCE outlier showed very strong signal pulsations, an effect that can be minimized by placing the arterial ROI on the descending aorta below the origin of the renal arteries (see supplementary file). In ASL, a possible

source of error is imperfect labelling in the aorta, leading to a signal drop in the label images. The patient data show several cases with very low RBF measurement in ASL, and HV's data show significant fluctuations between follow-ups in the same subject (see supplementary file). Inspection of the scans confirmed a global signal dropout in perfusion maps in these cases, consistent with the effect of reduced labelling efficiency due to B_0 inhomogeneity near the inversion plane (21). To mitigate this effect, a separate B_0 shimming at the labelling site will be considered for future acquisitions.

As noted above, both types of error can be addressed by improvements in the acquisition and/or analysis. An alternative strategy would be to combine all three methods, either by reporting the median value or performing a joint optimization (22). Alternatively, PC can be used to derive global RBF values, while ASL and DCE can be employed to determine spatial heterogeneity in perfusion but not absolute values. For the repeatability study, we reported RRE which relates to the coefficient of variation (CV) reported in other studies as $CV = RRE/1.96$. The repeatability of PC was in agreement with previous studies in the literature. In spite of the relatively long interval to complete four repeat scans (4 months on average), it was encouraging to find RRE of 11% (CV= 6%). This indicates that possible sources of variability such as difficulties in positioning the PC plane or the effect of free breathing were relatively small. The repeatability of PC-RBF in this study is comparable to the results reported by Dambreville et al. and Khatir et al. where two scans were acquired within one week with RRE of 17% and 16%, respectively.

Studies reporting repeatability for ASL using pCASL are very limited. One study reported short-term RRE of 27% for cortical perfusion using pCASL based on two scans acquired within the same visit (23). The RRE of ASL in our study (CV 31%) is

in agreement with the results reported by Harteveld et al. using the same pCASL labelling (24). Repeatability error in ASL of our study, however, is higher compared to previous studies using flow-sensitive alternating inversion recovery (FAIR) labelling approach (25,26). Besides the sensitivity to B_0 inhomogeneity, pCASL labelling can also be influenced by the maximum pulsatility and blood flow velocity of the descending aorta (27). Previous studies have reported a difference in RBF between healthy controls and patients with impaired renal function in the range between 90 and 470 mL/min (28,29). Thus, the current uncertainty in pCASL labelling would indicate that subtle changes in RBF (due to disease progression or follow-up responses after interventions) may go undetected.

Absolute RBF values in this study are comparable to those reported by Khatir et al. (30) in healthy subjects and Jin et al. using breath hold PC (31), Gillis et al. (28) and Shirvani et al. (32) using ASL with FAIR labelling and Rankin et al. (33) using the same pCASL labelling used in our study. Nevertheless, it is surprising that mean RBF of our healthy participants was substantially lower than reference values in the literature. Based on early work using the clearance of para-aminohippurate (PAH), normal RBF was determined to be 1129 mL/min/1.73 m^2 in healthy young subjects (34). These estimates agree with those of other studies using radioisotopes (35). The population of HVs in our study was predominantly female, but while this will likely explain a small part of the difference with male cohorts (36), the effect of sex alone is insufficient to explain the large difference. Smaller RBF values are expected in diabetic patients (37), but the cohort in our study was at an early disease stage, and had values comparable to the HVs. A systematic underestimation is theoretically possible, but it is highly unlikely that ASL, DCE and PC would produce a broadly similar systematic error. A possible explanation lies in the effect of subject

preparation. For reasons related to the blood sampling in the iBEAt study, study participants were scanned after an overnight fast followed by a standardized breakfast and a drink of water immediately before the MRI. The content of the meal was chosen to avoid protein/salt rich food that is known to influence RBF, but a reduced RBF is consistent with the effect of fasting (38). A future study is currently being planned for, to help determine if this effect alone is sufficient to explain the lower RBF values found in this study.

Limitations

The acquisition order of PC, ASL and DCE was not randomized, due to the use of gadolinium contrast agent. PC was always acquired first as part of a multiparametric MRI protocol, resulting in a time difference of approximately 20 minutes between sequences. However, it is unlikely that this time difference could explain the differences observed between methods. While employing PC as a reference method has enriched the results of this study, there is a clear advantage of using other available methods such as ^{15}O-labeled water positron emission tomography (PET) imaging. This will be addressed in a separate cohort of iBEAt participants (14). The use of kidney volume to derive RBF from ASL and DCE may have introduced an additional source of variability to the measurements. This effect is expected to be small, however, since volume measurements derived from the same ROI were used for each technique. The number of participants is small (n=25), and this is likely insufficient to detect the relatively small differences in the mean values between the three methods. Patient repeatability data was not available for this study, and repeatability values from healthy volunteers do not necessarily translate to disease due for instance to reduced cortico-medullary differentiation. Finally, despite efforts

in standardizing patient preparation, subtle physiological changes between the repeat scans could not be excluded.

Conclusions

Comparing RBF derived from ASL, DCE and PC showed little bias, but poor precision reflecting substantial differences at the individual level. Triangulation with PC indicated that ASL and DCE can achieve a comparable level of accuracy.

REFERENCES

1. Burke M, Pabbidi MR, Farley J, Roman RJ. Molecular mechanisms of renal blood flow autoregulation. Curr Vasc Pharmacol. 2014;12(6):845–858.
2. Cai Y-Z, Li Z-C, Zuo P-L, et al. Diagnostic value of renal perfusion in patients with chronic kidney disease using 3D arterial spin labelling. J Magn Reson Imaging. 2017;46(2):589–594.
3. Sourbron SP, Michaely HJ, Reiser MF, Schoenberg SO. MRI-measurement of perfusion and glomerular filtration in the human kidney with a separable compartment model. Invest Radiol. 2008;43(1):40–48.
4. Odudu A, Nery F, Harteveld AA, et al. Arterial spin labelling MRI to measure renal perfusion: a systematic review and statement paper. Nephrol Dial Transplant. 2018;33(suppl_2):ii15–21.
5. Su M-YM, Huang K-H, Chang C-C, et al. MRI evaluation of the adaptive response of the contralateral kidney following nephrectomy in patients with renal cell carcinoma. J Magn Reson Imaging. 2015;41(3):822–828.
6. Brown RS, Sun MRM, Stillman IE, et al. The utility of magnetic resonance imaging for noninvasive evaluation of diabetic nephropathy. Nephrol Dial Transplant Off Publ Eur Dial Transpl Assoc - Eur Ren Assoc. 2020;35(6):970–978.
7. Selby NM, Blankestijn PJ, Boor P, et al. Magnetic resonance imaging biomarkers for chronic kidney disease: a position paper from the European Cooperation in Science and Technology Action PARENCHIMA. Nephrol Dial Transplant. 2018;33(suppl_2):ii4–14.
8. Wu W-C, Su M-Y, Chang C-C, Tseng W-YI, Liu K-L. Renal perfusion 3-T MR imaging: a comparative study of arterial spin labelling and dynamic contrast-enhanced techniques. Radiology. 2011;261(3):845–853.
9. Cutajar M, Thomas DL, Hales PW, et al. Comparison of ASL and DCE MRI for the non-invasive measurement of renal blood flow: quantification and reproducibility. Eur Radiol. 2014;24(6):1300–1308.
10. Zimmer F, Zöllner FG, Hoeger S, et al. Quantitative renal perfusion measurements in a rat model of acute kidney injury at 3T: testing inter-and intramethodical significance of ASL and DCE-MRI. PLoS One. 2013;8(1).
11. Hockings P, Saeed N, Simms R, et al. MRI Biomarkers. In: Seiberlich N, Gulani V, Calamante F, Campbell-Washburn A, Doneva M, Hu HH, et al., editors. Quantitative Magnetic Resonance Imaging. 1st ed. Elsevier Academic Press; 2020. p. Iiii–Ixxxvi.
12. Villa G, Ringgaard S, Hermann I, et al. Phase-contrast magnetic resonance imaging to assess renal perfusion: a systematic review and statement paper. Magn Reson Mater Physics, Biol Med. 2020;33(1):3–21.
13. Eckerbom P, Hansell P, Cox E, et al. Multiparametric assessment of renal physiology in healthy volunteers using noninvasive magnetic resonance imaging. Am J Physiol Renal Physiol. 2019;316(4): F693–702.
14. Gooding KM, Lienczewski C, Papale M, et al. Prognostic Imaging Biomarkers for Diabetic Kidney Disease (iBEAt): Study protocol. BMC Nephrol. 2020;21(242).

15. Buxton RB, Frank LR, Wong EC, et al. A general kinetic model for quantitative perfusion imaging with arterial spin labelling. Magn Reson Med. 1998;40(3):383–396.

16. Sourbron S. plaresmedima/PMI-0.4-SUGAR: Outcomes [Internet]. 2020. Available from: https://zenodo.org/record/4086055

17. Buonaccorsi GA, O'Connor JPB, Caunce A, et al. Tracer kinetic model–driven registration for dynamic contrast-enhanced MRI time-series data. Magn Reson Med. 2007;58(5):1010–1019.

18. Dujardin M, Sourbron S, Luypaert R, Verbeelen D, Stadnik T. Quantification of renal perfusion and function on a voxel-by-voxel basis: A feasibility study. Magn Reson Med. 2005;54(4):841–849.

19. Du Bois D, Du Bois EF. Clinical Calorimetry: Tenth paper a formula to estimate the approximate surface area if height and weight be known. Arch Intern Med. 1916; XVII(6_2):863–871.

20. Bland JM, Altman DG. Statistical methods for assessing agreement between two methods of clinical measurement. Lancet (London, England). 1986;1(8476):307–310.

21. Wu W-C, Fernández-Seara M, Detre JA, Wehrli FW, Wang J. A theoretical and experimental investigation of the tagging efficiency of pseudocontinuous arterial spin labelling. Magn Reson Med. 2007;58(5):1020–1027.

22. Robson PM, Madhuranthakam AJ, Dai W, et al. Strategies for reducing respiratory motion artifacts in renal perfusion imaging with arterial spin labelling. Magn Reson Med. 2009;61(6):1374–1387.

23. Kim DW, Shim WH, Yoon SK, et al. Measurement of arterial transit time and renal blood flow using pseudocontinuous ASL MRI with multiple post-labelling delays: Feasibility, reproducibility, and variation. J Magn Reson Imaging. 2017;46(3):813–819.

24. Harteveld AA, de Boer A, Franklin SL, et al. Comparison of multi-delay FAIR and pCASL labelling approaches for renal perfusion quantification at 3T MRI. Magn Reson Mater Physics, Biol Med. 2020;33(1):81–94.

25. Cox EF, Buchanan CE, Bradley CR, et al. Multiparametric renal magnetic resonance imaging: validation, interventions, and alterations in chronic kidney disease. Front Physiol. 2017; 8:696.

26. de Boer A, Harteveld AA, Stemkens B, et al. Multiparametric Renal MRI: An Intrasubject Test–Retest Repeatability Study. J Magn Reson Imaging. 2020; 53(3):859-873.

27. Amanuma M, Mohiaddin RH, Hasegawa M, Heshiki A, Longmore DB. Abdominal aorta: characterisation of blood flow and measurement of its regional distribution by cine magnetic resonance phase-shift velocity mapping. Eur Radiol. 1992;2(6):559–564.

28. Gillis KA, McComb C, Patel RK, et al. Non-Contrast Renal Magnetic Resonance Imaging to Assess Perfusion and Corticomedullary Differentiation in Health and Chronic Kidney Disease. Nephron. 2016;133(3):183–192.

29. Buchanan CE, Mahmoud H, Cox EF, et al. Quantitative assessment of renal structural and functional changes in chronic kidney disease using multi-parametric magnetic resonance imaging. Nephrol Dial Transplant. 2019; 35(6):955-964.

30. Khatir DS, Pedersen M, Jespersen B, Buus NH. Reproducibility of MRI renal artery blood flow and BOLD measurements in patients with chronic kidney disease and healthy controls. J Magn Reson Imaging. 2014;40(5):1091–1098.

31. Jin N, Lewandowski RJ, Omary RA, Larson AC. Respiratory self-gating for free-breathing abdominal phase-contrast blood flow measurements. J Magn Reson Imaging. 2009;29(4):860–868.

32. Shirvani S, Tokarczuk P, Statton B, et al. Motion-corrected multiparametric renal arterial spin labelling at 3 T: reproducibility and effect of vasodilator challenge. Eur Radiol. 2019; 29(1):232–420.

33. Rankin AJ, Allwood-Spiers S, Lee MMY, et al. Comparing the interobserver reproducibility of different regions of interest on multi-parametric renal magnetic resonance imaging in healthy volunteers, patients with heart failure and renal transplant recipients. MAGMA. 2020; 33(1).

34. Davies DF, Shock N. Age changes in glomerular filtration rate, effective renal plasma flow, and tubular excretory capacity in adult males. J Clin Invest. 1950;29 5:496–507.

35. Botti RE, Razzak MA, MacIntyre WJ, Pritchard WH. The relationship of renal blood flow to cardiac output in normal individuals as determined by concomitant radioisotopic measurements. Cardiovasc Res. 1968; 2(3):243–246.

36. Bax L, Bakker CJG, Klein WM, et al. Renal blood flow measurements with use of phase-contrast magnetic resonance imaging: normal values and reproducibility. J Vasc Interv Radiol. 2005;16(6):807–814.

37. Mora-Gutierrez JM, Garcia-Fernandez N, Slon Roblero MF, et al. Arterial spin labelling MRI is able to detect early hemodynamic changes in diabetic nephropathy. J Magn Reson Imaging. 2017; 46(6):1810–1817.

38. Hostetter TH. Human renal response to meat meal. Am J Physiol. 1986;250(4 Pt 2): F613-618.

TABLES

Table 1 Summary of acquisition parameters for phase contrast (PC), arterial spin labelling (ASL) and dynamic contrast enhanced (DCE) MRI sequences.

MRI sequence	Scanning parameters
Phase contrast (PC)	Acquisition plane: sagittal; Acquisition mode: free breathing with ECG triggering; Pulse sequence: 2D gradient echo; FOV 350 x 241 mm; TR 40.48 ms; TE 2.74 ms; FA 25°; voxel size 0.6×0.6 mm; Slice thickness 6 mm; velocity encoding 120 cm/sec; Acquisition time: 1:40 minutes.
Arterial spin labelling (ASL)*	Acquisition plane: Coronal-oblique; Acquisition mode: free breathing; Readout: 3D TGSE; FOV 300x150 mm; TR 5000 ms; TE 19.28 ms; excitation FA 90°; slice thickness 5 mm; Number of slices 16 Labelling scheme: pCASL; labelling duration 1500 ms; post-labelling delay 1500 ms.
Dynamic contrast enhanced (DCE)	Acquisition plane: 8 Coronal-oblique slices and 1 transverse slice; Acquisition mode: free breathing; Pulse sequence: 2D Turbo-FLASH; FOV 400x400 mm; TR 179 ms; TE 0.97 ms; FA 10°; TI 85 ms; slice thickness 7.5 mm; temporal resolution 1.6 sec; parallel imaging: GRAPPA 2; Acquisition time: 7:07 minutes.

***** Work-In-Progress package, the product is currently under development and is not for sale in the US and in other countries. Its future availability cannot be ensured.

ECG: Echocardiogram; FA: flip angle; FLASH: fast low angle shot; FOV: field of view; pCASL: pseudo-continuous arterial spin labelling; TE: echo time; TI: inversion time; TR: repletion time; TGSE: Turbo gradient spin echo.

Table 2 The mean and 95% confidence interval (CI) and Pearson's correlation coefficient calculated with and without outliers for renal blood flow measurement in diabetic patients.

MRI technique	Outlier included (n=25)	Outlier removed (n=24)
Mean ± 95% CI (mL/min/1.73 m^2)		
PC	618± 62	618±64
ASL	526± 91	544± 88
DCE	569±110	525± 72
Pearson's correlation coefficient (*r*)		
PC-ASL	0.57‡	0.61‡
PC-DCE	0.34	0.57‡
DCE-ASL	-0.05	0.41‡

‡ Indicates significant correlation, $p<0.05$

ASL: arterial spin labelling; DCE: dynamic contrast enhanced; PC: phase contrast

Table 3 Summary statistics of repeatability results in RBF (mL/min/1.73 m^2) and split RBF measured with ASL and PC on healthy volunteers.

	RBF (mL/min/1.73 m^2)			**Split RBF**			
	mean ± 95% CI	RE ± 95% CI	RRE (%) ± 95% CI	mean ± 95% CI	RE ± 95% CI	RRE (%) ± 95% CI	***p*** **
PC	709± 130	79± 41	11± 6	0.54± 0.03	0.04± 0.02	6 ± 2.7	0.31
ASL	508± 202	241± 85	61± 19	0.50± 0.05	0.06± 0.04	11± 7.6	0.03
p *	0.13	0.02	0.06	0.22	0.35	0.22	

* *p*-value for PC vs ASL, ** *p*-value for the difference in RRE between RBF vs split RBF.

ASL: arterial spin labelling; CI: confidence interval; PC: phase contrast; RBF: renal blood flow; RE: repeatability error; RRE: relative repeatability error

FIGURES

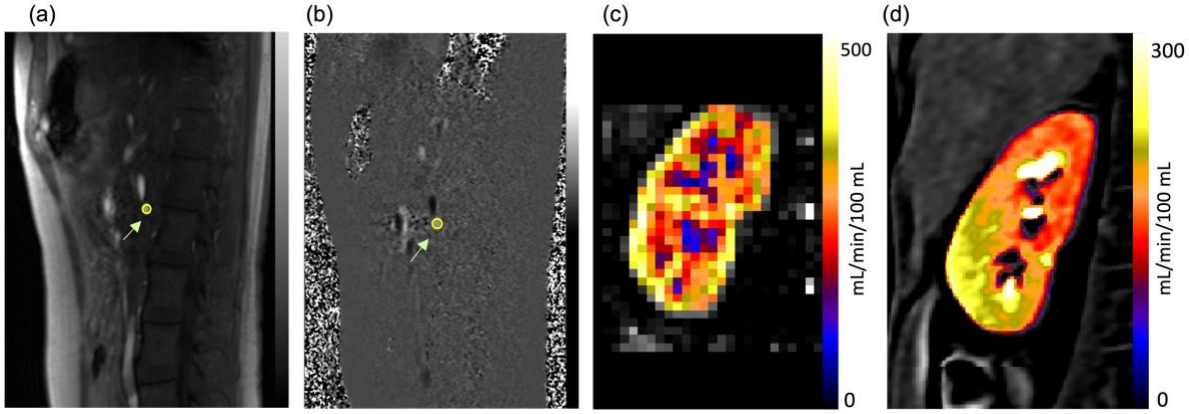

Figure 1 Representative image showing the region-of-interest (ROI) placement on phase contrast (PC) magnitude and velocity images (a and b, respectively), arterial spin labelling (ASL) perfusion map (c), and dynamic contrast enhance (DCE) apparent extracellular volume map (d).

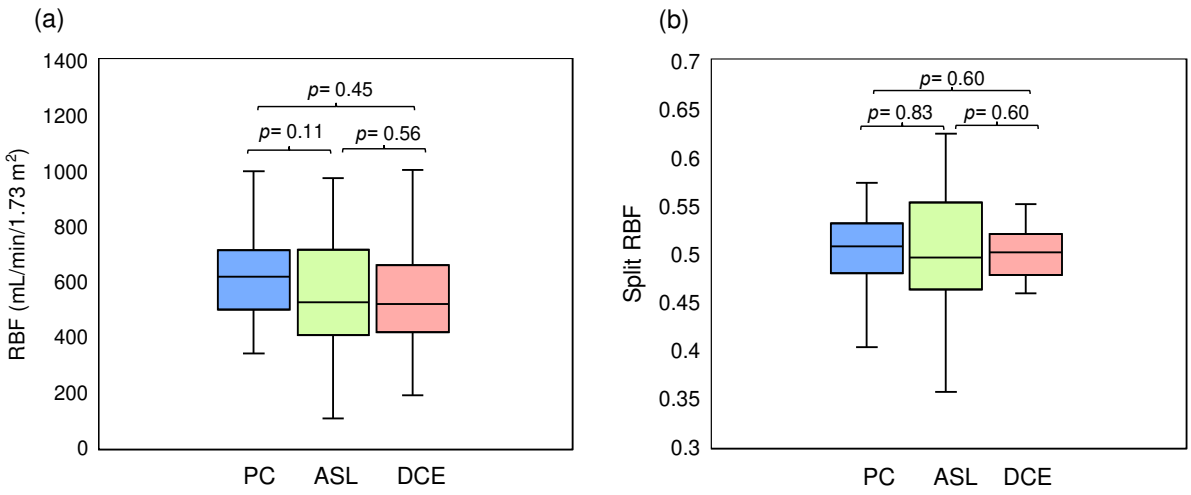

Figure 2 Box and whisker plots depicting distribution of renal blood flow (RBF) (a) and split RBF (b) measured with phase contrast (PC), arterial spin labelling (ASL) and dynamic contrast enhanced (DCE). The p-values for pairwise comparisons of means are given above the plots.

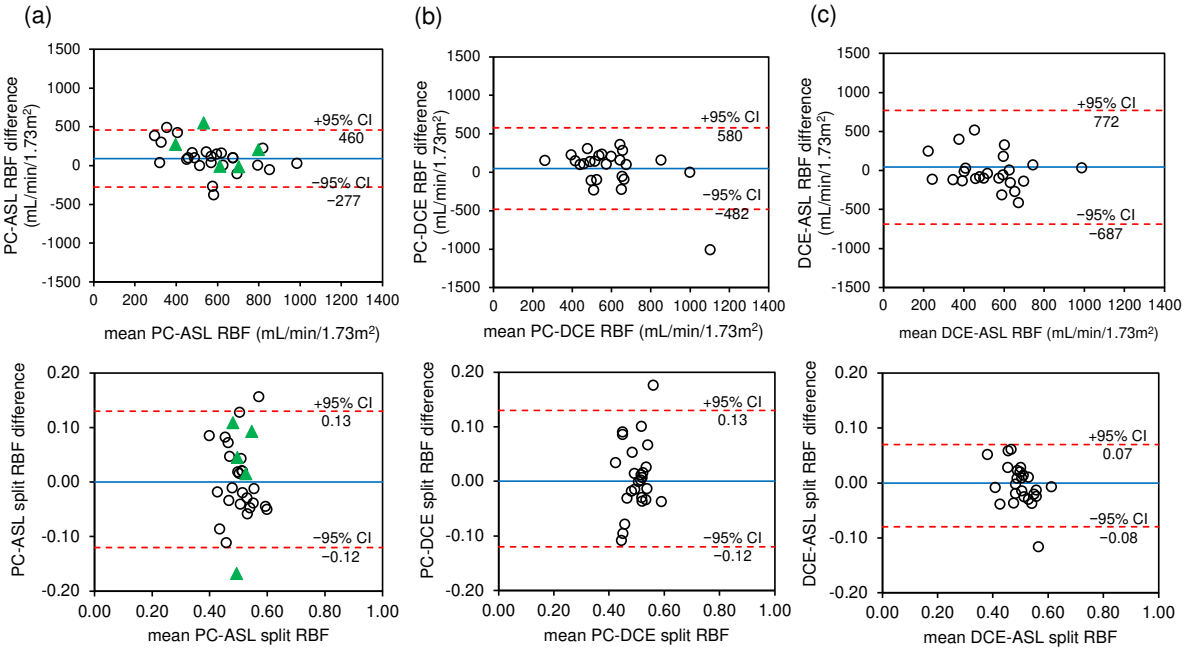

Figure 3 Bland-Altman plots comparing phase contrast, arterial spin labelling (PC-ASL) (a), phase contrast, dynamic contrast enhanced (PC-DCE) (b) and DCE-ASL (c) for renal blood flow (RBF) (top panel) and split-RBF (bottom *panel)*. Dashed lines indicate upper and lower 95% confidence intervals (CI) calculated as: mean difference ± 1.96 (SD). Solid lines represent the mean difference between two techniques. Measurement of ASL-PC in healthy volunteers (▲) were plotted for visual reference.

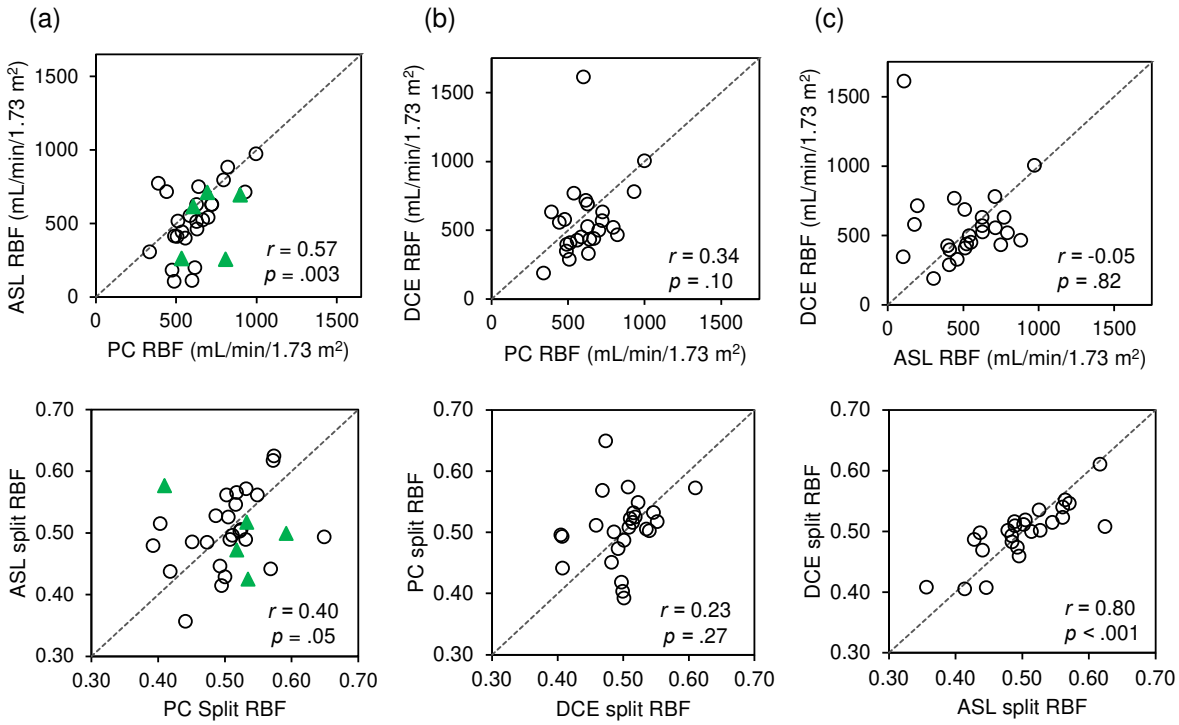

Figure 4 Scatterplots for phase contrast (PC) and arterial spin labelling (ASL) (a); PC and dynamic contrast enhanced (DCE) (b); ASL and DCE (c), for renal blood flow (RBF) (top panel) and Split-RBF (bottom panel) for diabetic patients (○). Pairwise Pearson's correlation (r) and p-value for the significance of the correlation are shown in the plots. The dotted line is the identity. Measurements of ASL-PC in healthy volunteers (▲) were plotted for visual reference

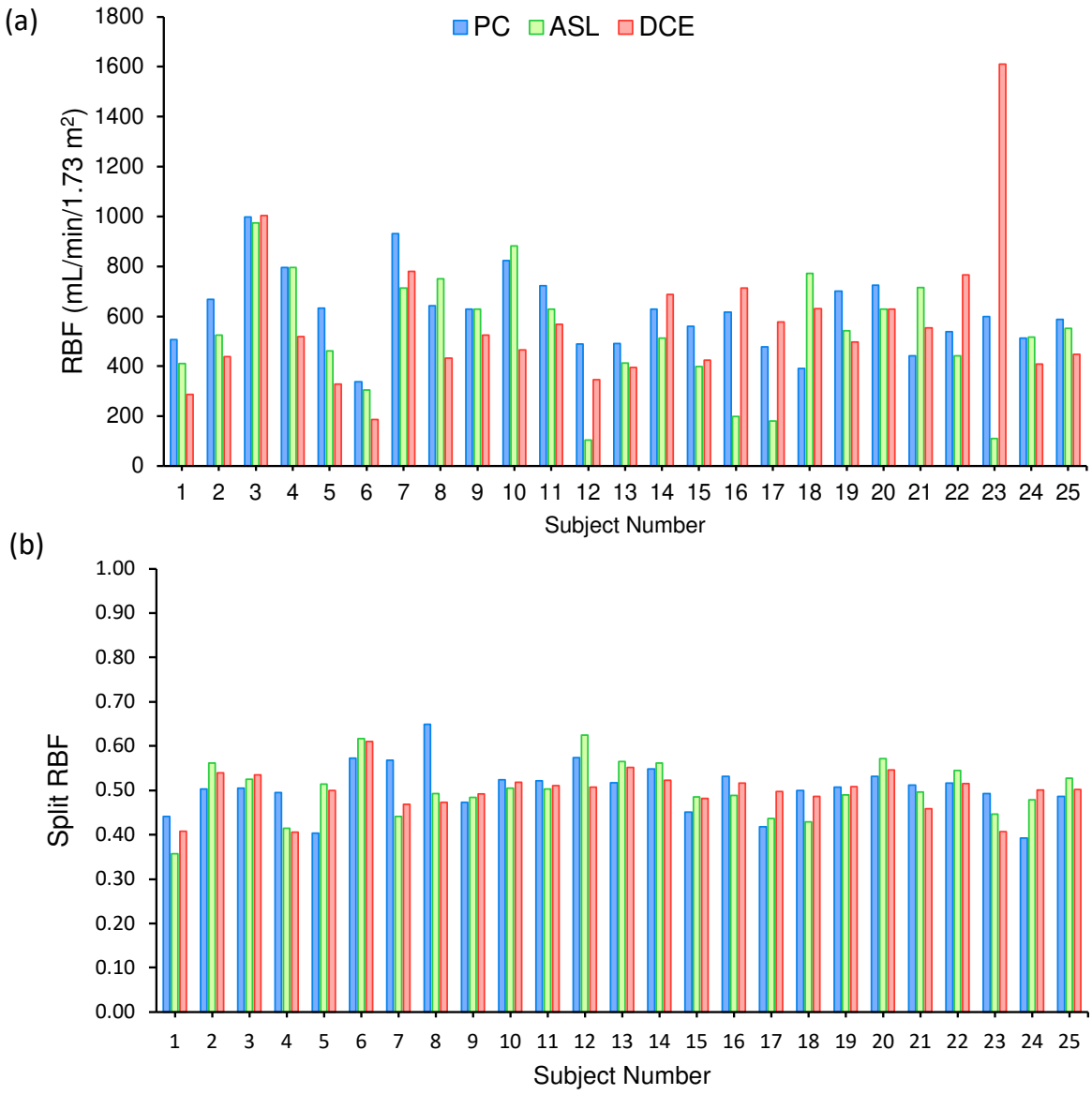

Figure 5 Bar chart for renal blood flow (RBF, ml/min/1.73 m2) (top row) and split-RBF (bottom row) for all patients (1-25, horizontal axis) and each of the three methods (color-coded).

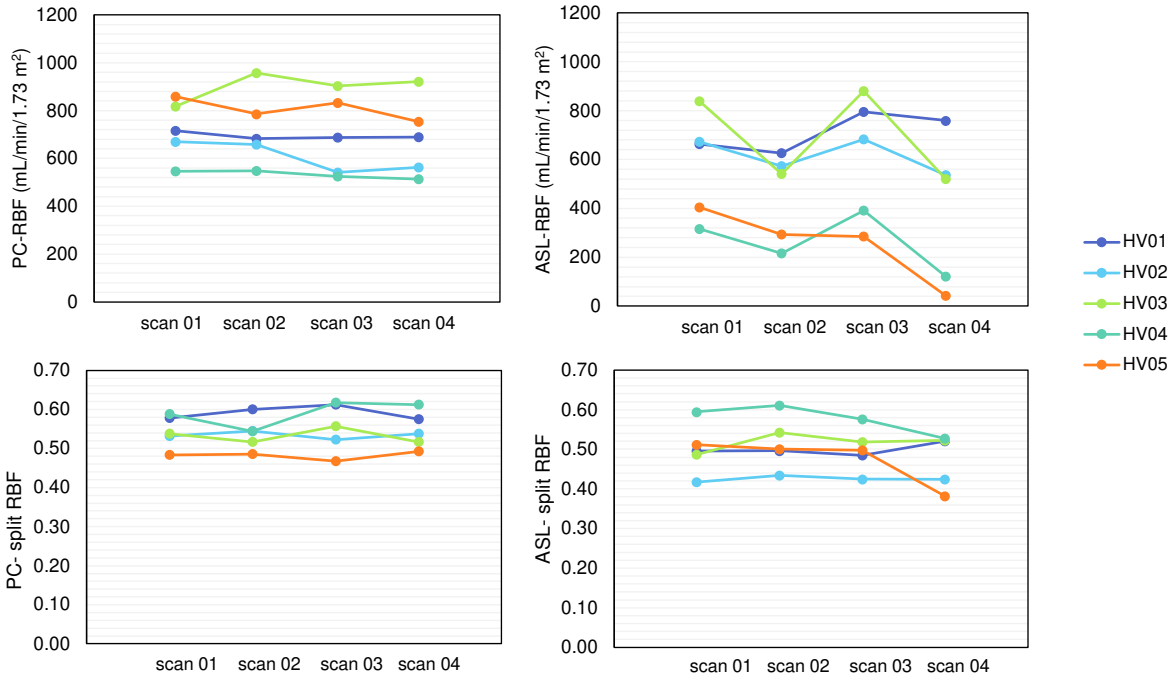

Figure 6 Repeat measurements of renal blood flow (RBF) (top row) and split RBF (bottom row) for each of the five healthy volunteers (HV 01 to HV 05 color coded) derived from phase contrast (PC) (left) and arterial spin labelling (ASL) (right).